Acta Pharmacologica Sinica

www.nature.com/aps

ARTICLE

Deficiency of β-arrestin2 exacerbates inflammatory arthritis by facilitating plasma cell formation

Wei-jie Zhou[1], Dan-dan Wang[1], Juan Tao[1], Yu Tai[1], Zheng-wei Zhou[1], Zhen Wang[1], Pai-pai Guo[1], Wu-yi Sun[1], Jing-yu Chen[1], Hua-xun Wu[1], Shang-xue Yan[1], Ling-ling Zhang[1], Qing-tong Wang[1] and Wei Wei[1]

β-arrestin2 (β-arr2) is, a key protein that mediates desensitization and internalization of G protein-coupled receptors and participates in inflammatory and immune responses. Deficiency of β-arr2 has been found to exacerbate collagen antibody-induced arthritis (CAIA) through unclear mechanisms. In this study we tried to elucidate the molecular mechanisms underlying β-arr2 depletion-induced exacerbation of CAIA. CAIA was induced in β-arr2$^{-/-}$ and wild-type (WT) mice by injection of collagen antibodies and LPS. The mice were sacrificed on d 13 after the injection, spleen, thymus and left ankle joints were collected for analysis. Arthritis index (AI) was evaluated every day or every 2 days. We showed that β-arr2$^{-/-}$ mice with CAIA had a further increase in the percentage of plasma cells in spleen as compared with WT mice with CAIA, which was in accordance with elevated serum IgG1 and IgG2A expression and aggravating clinical performances, pathologic changes in joints and spleen, joint effusion, and joint blood flow. Both LPS stimulation of isolated B lymphocytes in vitro and TNP-LPS challenge in vivo led to significantly higher plasma cell formation and antibodies production in β-arr2$^{-/-}$ mice as compared with WT mice. LPS treatment induced membrane distribution of toll-like receptor 4 (TLR4) on B lymphocytes, accordingly promoted the nuclear translocation of NF-κB and the transcription of Blimp1. Immunofluorescence analysis confirmed that more TLR4 colocalized with β-arr2 in B lymphocytes in response to LPS stimulation. Depletion of β-arr2 restrained TLR4 on B lymphocyte membrane after LPS treatment and further enhanced downstream NF-κB signaling leading to additional increment in plasma cell formation. In summary, β-arr2 depletion exacerbates CAIA and further increases plasma cell differentiation and antibody production through inhibiting TLR4 endocytosis and aggravating NF-κB signaling.

Keywords: rheumatoid arthritis; β-arrestin2; TLR4; plasma cell; B lymphocytes; LPS

Acta Pharmacologica Sinica (2021) 42:755–766; https://doi.org/10.1038/s41401-020-00507-1

INTRODUCTION

Rheumatoid arthritis (RA), a common chronic inflammatory autoimmune disease, is characterized by joint inflammation, pannus formation, synovial hyperplasia, cartilage and bone destruction, which eventually lead to joint deformity and loss of function [1, 2]. In the clinic, early diagnosis of RA mainly depends on the erythrocyte sedimentation rate, rheumatoid factor (RF) levels, anti-cyclic citrullinated peptide (CCP) antibody levels and other laboratory indicators [3]. The levels of RF and other specific autoantibodies decrease significantly after B lymphocyte clearance therapy, indicating the critical role of B lymphocytes in the pathogenesis of RA [4, 5]. In addition, B lymphocytes and plasma cells infiltrate into the synovium in RA patients. In RA, B lymphocytes stimulated by antigens develop and differentiate into memory B cells, and plasma cells ultimately secrete high-affinity antibodies [6]. These pathological autoantibodies then attack self-tissues, cause antibody-mediated immune responses involving multiple organs, induce damage to the body, causing the occurrence and development of RA [7]. Therefore, activation of B lymphocytes, overcloning of plasma cells, and production of a large amount of autoantibodies are important therapeutic targets for RA.

It has been reported that Toll-like receptor 4 (TLR4)-triggered signaling plays a pivotal role in the differentiation of B lymphocytes into plasma cells. TLR4 is an important receptor that transduces the response to lipopolysaccharide (LPS), which is a well-known B lymphocyte mitogen [8]. Classical animal models of RA, including models of adjuvant-induced arthritis, collagen-induced arthritis and collagen antibody-induced arthritis (CAIA), are induced by injection of LPS or bacille calmette-guerin into experimental animals to activate TLR4-mediated signaling, confirming the initial effect of TLR4 in aggravating the occurrence and development of autoimmune diseases [9]. TLR4-mediated activation and differentiation of B lymphocytes occur mainly through activation of the downstream nuclear factor-κB (NF-κB) signaling pathway. When the TLR4 receptor is stimulated by its ligands, tumor necrosis factor receptor-associated factor 6 and interleukin-1 receptor-associated kinase1/4 are recruited to myeloid differentiation factor 88 and subsequently activate transforming growth factor-β-activation kinase 1, which promotes the activity of the

[1]Institute of Clinical Pharmacology, Anhui Medical University, Key Laboratory of Anti-Inflammatory and Immune Medicine, Ministry of Education, Anhui Collaborative Innovation Center of Anti-Inflammatory and Immune Medicine, Hefei 230032, China
Correspondence: Qing-tong Wang (hfwqt727@163.com) or Wei Wei (wwei@ahmu.edu.cn)
These authors contributed equally: Wei-jie Zhou, Dan-dan Wang, Juan Tao, Yu Tai

Received: 15 May 2020 Accepted: 6 August 2020
Published online: 27 August 2020

inhibitor of NF-κB (IκB) kinase (IKK) family. Activated IKKs therefore phosphorylate and degrade IκB, leading to the nuclear translocation of NF-κB and the initiation of Blimp-1 transcription [10]. The transcription factor Blimp-1, also called the master regulator of the ultimate differentiation of B lymphocytes, controls the differentiation of B lymphocytes into plasma cells and the secretion of antibodies. Therefore, it is of great significance to reduce the membrane distribution of TLR4 for signal termination and immune balance maintenance.

Accumulating data have shown that TLR4 can be internalized upon LPS stimulation and that this endocytosis negatively regulates inflammation [11]. However, the process of TLR4 endocytosis needs to be explored. Notably, β-arrestin (β-arr) is a key protein that mediates the desensitization and internalization of the largest receptor family, the G protein-coupled receptor (GPCR) family, by interfering with the binding of GPCRs to specific G proteins and recruiting clathrin to form clathrin-coated vesicles [12, 13]. In addition to interacting with GPCRs, β-arr works as a powerful scaffolding protein that interacts with over 400 non-GPCR protein partners to transduce multiple downstream signals. Furthermore, other types of receptors, including receptor tyrosine kinases and nuclear receptors, have been demonstrated to be targets of β-arr [14, 15]. β-arr2 is widely expressed in various mammalian tissues and immune cells, especially lymphocytes, and is involved in the negative regulation of the immune response [16]. A previous study revealed exacerbation of arthritis accompanied by more severe arthritis index and paw swelling and more obvious pathological changes in the joints in β-arr2 knockout (β-arr2$^{-/-}$) mice with CAIA than that in WT mice with CAIA, suggesting that β-arr2 has a notably protective effect against arthritis; however, the underlying mechanism needs to be clarified [17]. In the present work, we found that the percentage of plasma cells in the spleens of β-arr2$^{-/-}$ mice with CAIA was significantly higher than that in the spleens of WT mice with CAIA, suggesting that β-arr2 participates in the differentiation of plasma cells. Furthermore, we present evidence that β-arr2 inhibits the excessive formation of plasma cells in inflammatory arthritis by regulating TLR4 and its downstream signaling.

MATERIALS AND METHODS

Animals

Male β-arr2$^{-/-}$ mice on the C57BL/6J background were obtained from Jackson Laboratory (stock No. 011130, Bar Harbor, ME, USA). The β-arr2$^{-/-}$ strain was created with a 129-derived embryonic stem cell line by deleting exon 2 of the β-arr2 gene on chromosome 11. β-arr2$^{-/-}$ homozygous and WT littermates were used for the indicated experiments. An image of a gel used for genotyping is presented in Supplementary Fig. S1. Male C57BL/6J mice (18 ± 2 g) (certificate number: SCXK (Su) 2016-0010) were obtained from Changzhou Cavens Experimental Animals Co., Ltd. All mice were raised in the SPF animal laboratory at Anhui Medical University, and the experiments were approved by the Ethical Review Committee of Animal Experiments, Institute of Clinical Pharmacology, Anhui Medical University, according to the guidelines of the Helsinki Declaration (certificate No. LLSC2013007).

Reagents

A cocktail of five monoclonal antibodies against type II collagen was purchased from Chondrex, Inc. (Redmond, WA, USA). Mouse CD19-APC, CD19-FITC, CD138-PE and CD27-PE antibodies for flow cytometry were obtained from BD Biosciences (Franklin Lakes, NJ, USA). A monoclonal antibody against TLR4 (Cat#: sc-293072) was purchased from Santa Cruz Biotechnology (Dallas, TX, USA). Goat anti-β-arr2 (Cat#: ab31294) and rabbit anti-NF-κB p65 (Cat#: ab16502) antibodies were obtained from Abcam (Cambridge, MA, USA). A mouse monoclonal ATPase Na^+/K^+ transporting subunit alpha 1 (ATP1A1) antibody (Cat#: TA309580) was purchased from ZSGB-BIO (Beijing, China). Rabbit anti-β-actin (Cat#: AF7018) and rabbit anti-GAPDH (Cat#: AF7021) primary antibodies, horseradish peroxidase (HRP)-conjugated goat anti-mouse IgG (H+L) (Cat#: S0002), goat anti-rabbit IgG (H+L) (Cat#: S0001) and rabbit anti-goat IgG (H+L) (Cat#: S0010) secondary antibodies were purchased from Affinity Biosciences (Cincinnati, OH, USA). Alexa Fluor 488 AffiniPure goat anti-mouse IgG (H+L) (Cat#: 115-545-062), Alexa Fluor Rhodamine Red AffiniPure donkey anti-goat IgG (H+L) (Cat#: 705-295-003) and Alexa Fluor 488 AffiniPure goat anti-rabbit IgG (H+L) (Cat#: 111-005-003) antibodies were purchased from Jackson ImmunoResearch Inc. (West Grove, PA, USA). Cell counting kit-8 (CCK-8) was obtained from Dojindo Molecular Technologies (Kumamoto, Japan). LPS (Cat#: L3024-10MG) and 2,4,6-trinitrobenzenesulfonic acid (TNP)-LPS (Cat#: T3382) were purchased from Sigma-Aldrich (Saint Louis, MO, USA). Magzol RNA extraction reagent was purchased from Invitrogen (Waltham, MA, USA). The HiScript II qRT SuperMix for qPCR kit and the SYBR Green Master Mix kit were purchased from Vazyme Biotech Co., Ltd. (Nanjing, China). Mouse IgG1 (Cat#: ELM-IGG1-1) and IgG2A (Cat#: ELM-IGG2A-1) ELISA test kits were obtained from Raybiotech (Norcross, GA, USA). RPMI-1640 and DMEM were obtained from Biological Industries (Cromwell, CT, USA).

Collagen antibody-induced arthritis mouse model

As previously described, to induce a high occurrence of arthritis, a cocktail of five monoclonal antibodies against type II collagen (5 mg/mouse) was intraperitoneally injected on day 0, and then LPS (50 μg/mouse) was intraperitoneally injected on day 3. Control mice were injected with an equivalent volume of saline. Arthritis developed on day 4, and inflammation peaked on days 8–9 [18].

TNP-LPS induced an inflammatory immune response in mice

The murine humoral immune response was induced by intraperitoneal injection of TNP-LPS (15 μg/mice) into WT C57BL/6J or β-arr2$^{-/-}$ mice on day 0. The mice were sacrificed on day 14 after injection, and the proportion of splenic plasma cells as well as the serum levels of IgG1 and IgG2A antibodies was determined.

Evaluation of arthritis

To evaluate the severity of arthritis, two independent observers blinded to the groups recorded body weight, the number of swollen joints, and the arthritis index (AI) every day or every 2 days as previously reported [19]. The structure (acquired in B-mode) and blood flow (acquired by color Doppler) of the left knee joint of each mouse were detected with a Vevo 2100 Ultrasound Imaging System (FUJIFILM VisualSonics Inc., Toronto, Canada) using an MS550 probe at the peak inflammation period. The dark area of the joint was graded from 0 to 4, and blood signaling was graded from 0 to 3 based on the severity of changes relative to the characteristics of the normal knee joint [20].

Organ collection and histopathological examination

Mice were weighed, anesthetized and sacrificed, and the spleen and thymus of each mouse were removed and weighed. The spleen and thymus indexes were calculated by comparing the weight of each organ with body weight. The left ankle joints and spleen were removed and fixed with 4% formalin. After 24 h of fixation, the ankle joints were decalcified in 10% ethylenediaminetetraacetic acid until soft. The ankles and spleens were embedded in paraffin and cut into 5-μm sections for hematoxylin and eosin (H&E) staining. Histopathological changes in inflammation, pannus, bone erosion, cell infiltration, and synovial hyperplasia in the ankle slides were quantified. The number of germinal centers, cell density of the lymphatic sheath, area of the marginal zone and red pulp, and degree of lymphoid follicular hyperplasia were graded based on histopathological examination of the spleen as previously described [21].

B lymphocyte isolation
Lymphocytes were extracted from the spleen by density gradient centrifugation and resuspended in PBS at a concentration of 1×10^9 cells/mL. Splenic lymphocytes were labeled with the B lymphocyte surface marker CD19 (APC-conjugated) and incubated in the dark for a half hour at 4 °C. The samples were then sorted with a flow sorter (BD FACS Aria) to purify B lymphocytes (Supplementary Fig. S2).

Analysis of the percentages of plasma cells and memory B cells in the spleens of mice and the expression of TLR4 on the B lymphocyte membrane by flow cytometry
The spleens of the mice were removed and separated mechanically, and lymphocytes were isolated in lymphocyte separation medium. Splenic lymphocytes were transferred to a 12-mm × 75-mm flow cytometry tube and incubated with an APC-conjugated CD19/PE-conjugated CD138 antibody mixture or an FITC-conjugated CD19/PE-conjugated CD27 antibody mixture. The samples were sufficiently mixed and incubated at 4 °C for 30 min in the dark. B lymphocyte labeling was analyzed by flow cytometry (FC500, Beckman Coulter Life Sciences, Fullerton, CA, USA) or on an Amnis imaging flow cytometer (Luminex Corporation, Austin, TX, USA). The percentage of B lymphocyte subsets was analyzed using CellQuest™ software (BD, San Diego, CA, USA). To detect the specific expression of TLR4 on the membranes of B lymphocytes, isolated splenic lymphocytes were first labeled with an APC-conjugated anti-CD19 antibody before fixation without permeabilization. The B lymphocytes were then incubated with a primary TLR4 antibody for 1 h at room temperature and then with an Alexa Fluor 488-conjugated secondary antibody for a half hour. Cells labeled only with secondary antibody served as negative controls. All the samples were tested with a flow cytometer, and the mean fluorescent intensity of TLR4 was compared.

Analysis of the colocalization of TLR4 and β-arr2 and NF-κB nuclear translocation by immunofluorescence
Sorted splenic B lymphocytes were fixed with 4% (w/v) buffered paraformaldehyde for 15 min at room temperature. Subsequently, they were permeated with 0.1% Triton X-100 for 30 min and blocked for 30 min in 1% BSA-PBS. Each group of cells was incubated with a mouse anti-TLR4, goat anti-β-arr2 or rabbit anti-NF-κB antibody overnight at 4 °C, washed with PBS three times, and incubated in the dark with an Alexa Fluor 488 AffiniPure goat anti-mouse IgG (H+L), Alexa Fluor 488 AffiniPure goat anti-rabbit IgG (H+L) or Alexa Fluor Rhodamine Red AffiniPure monkey anti-goat IgG (H+L) antibody for 2 h. The nuclei were stained with DAPI for 30 min and washed with PBS three times. Finally, cell smears were made on a clean microscope slide and sealed with a drop of antifluorescence quenching mounting solution. Digital images were obtained on a Leica TCS SP8 laser scanning confocal microscope. Colocalization of TLR4 and β-arr2 was analyzed using Leica LAS-AF software (version 4.0.0), and the average relative fluorescence intensity of nuclear NF-κB was quantified using ImageJ software (version 1.42q, NIH).

Analysis of the expression levels of β-arr2 and TLR4 and the expression of cytoplastic TLR4 by Western blotting
Splenic B lymphocytes were purified from different groups of mice and then lysed in cell lysis buffer with 10 mM PMSF and 10 mM phosphatase inhibitors on ice for 30 min. Soluble proteins were collected by centrifugation at 12,000 rpm for 30 min at 4 °C. The cytoplasmic proteins were further isolated by additional ultracentrifugation at 100,000 × *g* for 60 min at 4 °C. The purity of the cytoplasmic proteins was verified by blotting for ATP1A1. Denatured proteins combined with loading buffer were separated by SDS polyacrylamide gel electrophoresis and then transferred to PVDF membranes. The membranes were blocked with 5% nonfat milk in 0.05% Tween 20-PBS at 37 °C for 2 h. Primary antibodies against TLR4, β-arr2, β-actin, and GAPDH were used to blot specific proteins at 4 °C overnight. The membranes were then rinsed with TPBS three times and incubated with the corresponding secondary antibody at 37 °C for 2 h. The membranes were finally imaged on an ImageQuant LAS 500 imager (GE Healthcare Systems, Chicago, IL, USA) by applying ECL substrate, and the bands were semiquantified with ImageJ software.

Measurement of antibodies in the serum and cell culture supernatant by ELISA
The levels of IgG1 and IgG2A antibodies in the serum of mice from the different groups and the concentrations of autoantibodies in cell culture supernatants after in vitro treatment were measured by ELISA according to the manufacturer's instructions. Briefly, samples were plated in 96-well plates and incubated with IgG1 or IgG2A primary antibody followed by HRP-conjugated secondary antibody. The plate was read on a BioTek Elx × 808 microplate reader (BioTek, Winooski, VT, USA) at 450 nm, and the antibody concentrations in the samples were calculated using a standard curve.

Measurement of B lymphocyte vitality was by the CCK-8 assay
A total of 1×10^6 splenic B lymphocytes were seeded in each well of a 96-well plate and treated with LPS (final concentration of 5 mg/L) for 48 h in a 5% CO_2 cell incubator [12]. Two hours before the termination of culture, 10 μL of CCK-8 solution was added to each well, and the absorbance was determined on a BioTek Elx × 808 microplate reader at 450 nm.

The expression of Blimp1 mRNA was measured by real-time qPCR
The mRNA expression of Blimp1 was analyzed using real-time qPCR. In brief, splenic B lymphocytes were isolated and treated with LPS (20 mg/L) in vitro for 72 h to induce the differentiation of B lymphocytes [22]. Total RNA was extracted and then reverse transcribed into cDNA using reverse transcriptase. The cDNA templates were amplified according to the instructions of the SYBR Green Master Mix kit on a 7500 Real Time PCR System (Applied Biosystems, Foster City, CA, USA). Relative mRNA expression was quantified by the delta-delta CT method. The primer sequences for real-time qPCR were as follows: forward primer for Blimp1: 5′-TCCAGCACTGTGAGGTTTCA-3′, reverse primer for Blimp1: 5′-TCAAACTCAGCCTCTGTCCA-3′, forward primer for GAPDH: 5′-AGGTCGGTGTGAACGGATTTG-3′, reverse primer for GAPDH: 5′-TGTAGACCATGTAGTTGAGGTCA-3′.

Deposition of antibodies in the joints and spleen was measured by immunohistochemistry
Paraffin sections of ankle joint and spleen tissues were deparaffinized in xylene and rehydrated in ethanol. Subsequently, 0.5% Triton X-100 was used to permeabilize the tissue for 30 min. After rinsing in PBS, the sections were heated to boiling point for 10 min in citrate buffer (pH 6.0). Following incubation in hydrogen peroxide (3%) for 15 min, the slides were rinsed with PBS and incubated with polymer helper for 20 min at 37 °C. The sections were incubated with polyperoxidase-conjugated anti-mouse/rabbit IgG for 30 min at 37 °C was applied to label the antibodies that had accumulated in the tissues. After the sections were developed with 3,3′-diaminobenzidine tetrahydrochloride, they were counterstained with hematoxylin. All images were captured on a Leica DM1000 upright metallurgical microscope. The positive staining area was quantified with ImageJ software.

Statistical analysis
All data were analyzed by GraphPad Prism 6 statistical software and are expressed as the mean ± SD. Differences between multiple groups were evaluated by either one-way ANOVA with Tukey's posttest or two-way ANOVA with Sidak's posttest. A *t*-test

was applied to compare differences between two groups. $P < 0.05$ was considered significant.

RESULTS

β-arr2 depletion exacerbates CAIA in mice

To determine the function of β-arr2 in the process of inflammatory arthritis, a mixture of collagen antibodies was injected into β-arr2$^{-/-}$ and C57BL/6J WT mice to induce CAIA, and saline-injected mice were used as controls. Following antibody and LPS injection, the body weight gain of the mice consistently decreased from day 4. The loss of body weight was more severe in β-arr2$^{-/-}$ mice with CAIA than in WT mice CAIA, and there was a significant difference in body weight loss between β-arr2$^{-/-}$ mice with CAIA and WT mice with CAIA from day 8 after injection (Fig. 1a). Five days after antibody injection, the arthritis indexes (AIs) of both strains of mice with CAIA started to increase compared with the AI of control mice, and the paws were red and swollen. Inflammation peaked on approximately day 9–10 in both genotypes. Importantly, β-arr2$^{-/-}$ mice with CAIA exhibited more severe arthritis and a significantly higher AI than WT mice with CAIA from 8 days after injection (Fig. 1b). Similarly, β-arr2$^{-/-}$ mice with CAIA exhibited more swollen joints than WT mice with CAIA on days 5, 9, and 10 after antibody injection (Fig. 1c).

The joint cavity was observed as an inverted triangle structure formed between the femur, tibia and patellar ligament of the knee joint by ultrasonic imaging. The relative area of the dark liquid inside the cavity, which reflected the extension of effusion, was graded and analyzed. Almost no effusion was observed in control mice, whereas dark areas of different sizes were observed in the joints of mice with CAIA; however, the dark area in the joint cavities of β-arr2$^{-/-}$ mice with CAIA was much larger than that in the joint cavities of WT mice with CAIA, indicating that mice with CAIA and β-arr2 deficiency exhibited more severe inflammatory hydrarthrosis than mice with only CAIA (Fig. 1d, e). In addition, higher blood flow signals were found in the joints of mice with CAIA than in the joints of control mice by color Doppler. A relatively intense colored pattern was observed in β-arr2$^{-/-}$ mice with CAIA, although there was no significant difference between these mice and WT mice with CAIA (Fig. 1d, f). Unlike control mice, arthritic mice of both genotypes exhibited obvious splenomegaly and slight thymic atrophy. There was no significant difference in these symptoms between the β-arr2$^{-/-}$ and WT mice with CAIA (Fig. 1g, h). H&E staining showed that compared with those of control mice, the joints of both strains of CAIA mice exhibited obvious synovial inflammation, abundant inflammatory cell infiltration and pannus formation, severe synovial cell proliferation and bone and cartilage destruction. The pathological changes were graded, and the data revealed that β-arr2$^{-/-}$ mice with CAIA exhibited significantly higher scores for each parameter than WT arthritic mice (Fig. 1i, j). The spleens of both groups of mice with CAIA showed more germinal centers and lymphoid follicles, a larger marginal zone and red pulp area, and denser lymphatic sheaths than control mice. Importantly, depletion of β-arr2$^{-/-}$ aggravated the pathological changes in the germinal center, lymphoid follicular zone, marginal zone and red pulp (Fig. 1i, k). These data demonstrate that deficiency of the β-arr2 gene exacerbates murine inflammatory arthritis induced by collagen II antibodies and indicates that β-arr2 has a protective effect against these changes; nevertheless, the underlying mechanism remains to be determined.

β-arr2 depletion further increases plasma cell differentiation and antibody production in mice with CAIA

To evaluate the important function of humoral immunity in the pathogenesis of RA, we determined the percentages of splenic plasma cells, memory B cells and serum antibody levels in WT and β-arr2$^{-/-}$ mice with CAIA to investigate the pathological role of β-arr2 in arthritis. As expected, a substantial increase in the number of CD19^{-}CD138^{+} plasma cells was found in mice with CAIA regardless of genotype. There was a further increase the subpopulation of plasma cells in the spleens of β-arr2$^{-/-}$ mice with CAIA compared to the spleens of WT arthritic mice (Fig. 2a, c). The percentage of splenic CD19^{+}CD27^{+} memory B cells was upregulated in WT mice with CAIA and β-arr2$^{-/-}$ mice with CAIA compared with control mice, whereas there was no significant difference in the number of memory B cells between the two model groups (Fig. 2b, d). Serum IgG1 and IgG2A expression levels were greatly elevated in both groups of mice with CAIA, and there was a further increase in β-arr2$^{-/-}$ mice with CAIA compared to WT mice with CAIA (Fig. 2e, f). Immunohistochemical images showed that abundant IgG was deposited in joints and was expressed in splenic tissues in CAIA mice compared with normal controls of the same genotype. As expected, more IgG accumulated in β-arr2$^{-/-}$ mice with CAIA than in WT mice with CAIA (Fig. 2g, h). Together, these results reveal that the humoral immune response is stronger in arthritic mice lacking β-arr2 than in WT arthritic mice and that this stronger response may contribute to more severe inflammatory arthritis. However, the role of β-arr2 in plasma cell formation still needs to be elucidated.

β-arr2 depletion enhances TLR4-mediated signaling in B lymphocytes from mice with CAIA

As detected, β-arr2 expression was apparently increased in B lymphocytes from WT mice with CAIA compared with normal controls; however, the effect of β-arr2 expression on the development of B lymphocytes was not clearly shown (Fig. 3a). Since TLR4-mediated signaling is essential for B lymphocyte differentiation and activation, we evaluated the distribution of TLR4 in B lymphocytes from mice from the four groups. Membrane TLR4 expression was determined by flow cytometry, and the data showed that more TLR4 was distributed on the B lymphocyte membrane in mice with CAIA than in controls of the same genotype. Notably, even more TLR4 was found on B lymphocyte membrane from β-arr2$^{-/-}$ mice with CAIA than on those from WT arthritic mice (Fig. 3b). Cytosolic protein from B cells was separated by ultracentrifugation. Although TLR4 expression in the cytoplasm of B lymphocytes was obviously upregulated in both groups of CAIA mice compared to control mice, deficiency of β-arr2 substantially reduced the upregulated level of cytosolic TLR4. Moreover, our data showed that after protein fractionation, ATP1A1, which is a widely used reference marker for membrane fraction, was hardly detectable, suggesting that cytosolic protein isolation was successful (Fig. 3c). These data indicate that depletion of β-arr2 accelerates TLR4 membrane aggregation on inflammatory B lymphocytes; therefore, β-arr2 may be involved in endocytosis of TLR4 under immunostimulation. We further explored the interaction between β-arr2 and TLR4 in B lymphocytes upon immunization of WT mice in vivo, and a significant increase in the colocalization of these two molecules was observed in lymphocytes from mice with CAIA. Depletion of β-arr2 abolished this interaction in B lymphocytes from both normal mice and mice with CAIA (Fig. 3d). As expected, an abundance of NF-κB p65 translocated into the nuclei of splenic B lymphocytes from mice of both genotypes with CAIA, and nuclear NF-κB p65 expression in β-arr2$^{-/-}$ mice with CAIA mice was distinctly higher than that in WT mice with CAIA (Fig. 3e). This finding suggests that the absence of β-arr2 increases the expression of TLR4 of B lymphocyte membranes, therefore promoting the activity of NF-κB, the key signaling molecule downstream of TLR4 in B lymphocytes and promoting plasma cell formation in arthritis.

Loss of β-arr2 aggravates the TNP-LPS-induced humoral response in vivo

To verify the essential role of β-arr2 in inhibiting B lymphocyte differentiation and ultimately influencing humoral immunity, we

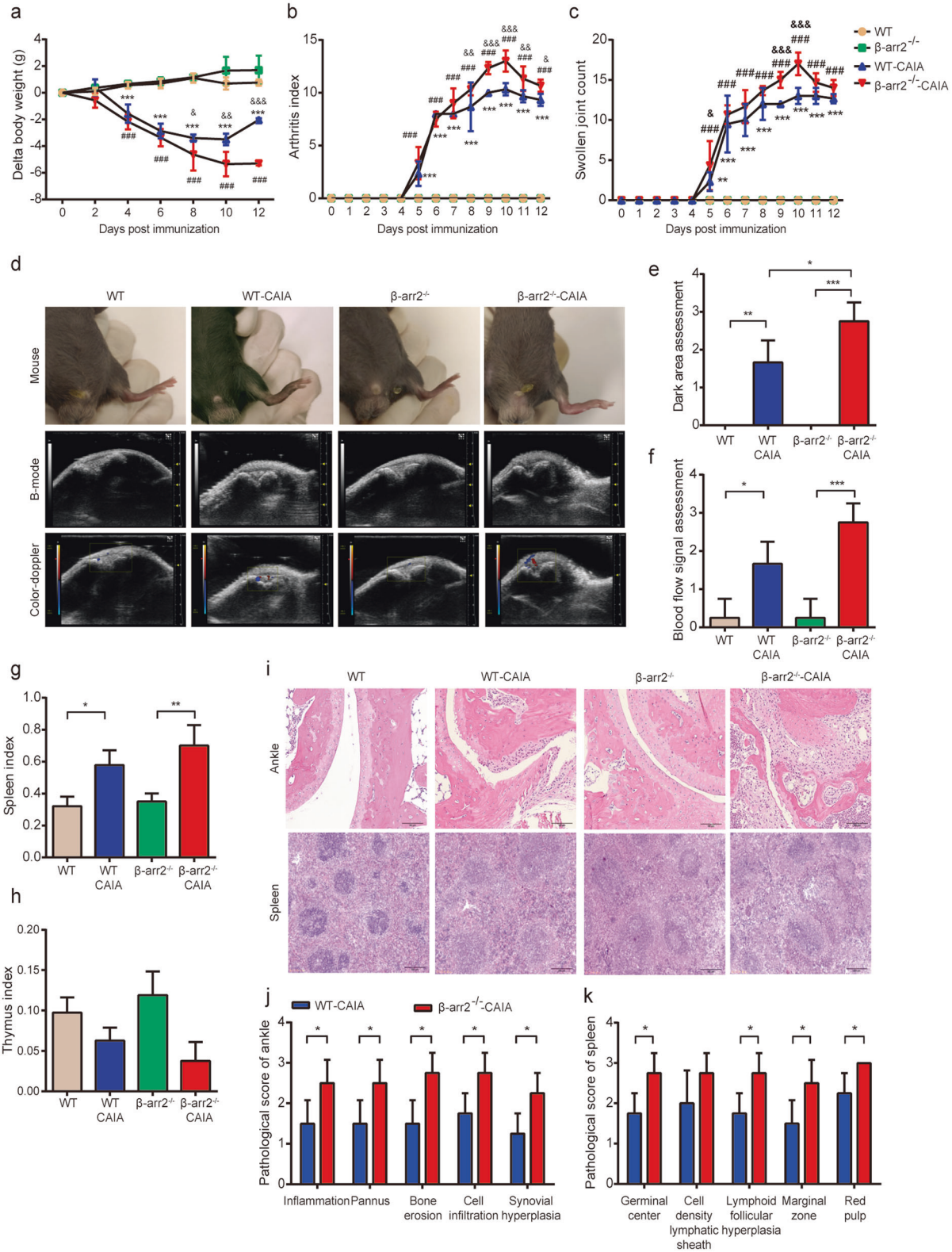

Fig. 1 β-arr2 depletion exacerbates CAIA in mice. **a** Body weight gain after the first injection (g). **b** Arthritis index. **c** Swollen joint count. **d** Representative images of the paws of mice from the different groups. Ultrasonic images of the knee joints in B-mode and by color Doppler. $^{**}P < 0.01$, $^{***}P < 0.001$, WT mice with CAIA vs WT control mice; $^{\#\#\#}P < 0.001$ β-arr2$^{-/-}$ mice with CAIA *vs* β-arr2$^{-/-}$ control mice; $^{\&}P < 0.05$, $^{\&\&}P < 0.01$, $^{\&\&\&}P < 0.001$ β-arr2$^{-/-}$ mice with CAIA *vs* WT mice with CAIA ($n = 8$). **e** The dark area in the joint cavity was assessed to reflect the severity of hydrarthrosis. **f** Blood flow signals were graded and analyzed. **g** The spleen index was calculated and is presented as the weight of the spleen in g/100g body weight. **h** The thymus index was calculated and is presented as the weight of the thymus in g/100g body weight. **i** Representative pathological images of the ankle (scale bar: 100 μm) and spleen (scale bar: 200 μm). **j** Pathological scores of the ankle were evaluated and analyzed. **k** Pathological scores of the spleen were graded and analyzed. $^{*}P < 0.05$, $^{**}P < 0.01$, $^{***}P < 0.001$ ($n = 5$).

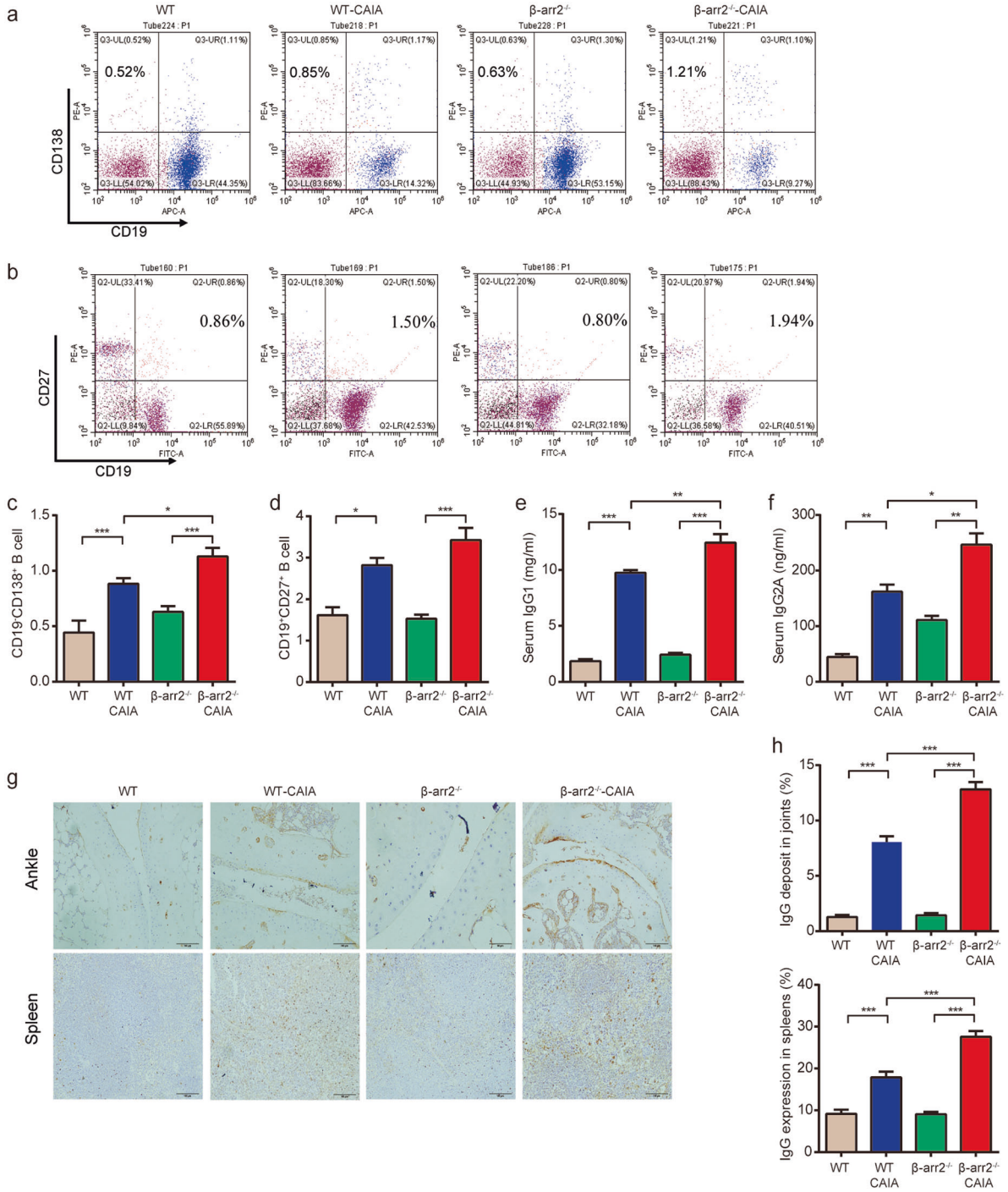

Fig. 2 β-arr2 depletion further increases plasma cell differentiation and antibody production in mice with CAIA. a Representative flow cytometry scatter plot of $CD19^{-}CD138^{+}$ splenic plasma cells. **b** Representative flow cytometry scatter plot of $CD19^{+}CD27^{+}$ splenic memory B cells. **c** The percentage of plasma cells was analyzed. **d** The percentage of memory B cells was analyzed. **e** Serum IgG1 levels (mg/mL) were determined by ELISA. **f** Serum IgG2A levels (ng/mL) were determined by ELISA. **g** Representative immunohistochemical images of IgG accumulation in the joints and spleen tissues. **h** The percentage of IgG deposition was measured by ImageJ software and analyzed. $^{*}P < 0.05$, $^{**}P < 0.01$, $^{***}P < 0.001$ ($n = 5$).

challenged β-arr2$^{-/-}$ homozygous mice and WT mice with TNP-conjugated LPS (TNP-LPS) and then investigated the T cell-independent B lymphocyte immune response to LPS [23]. Fourteen days after TNP-LPS injection, the percentage of plasma cells was determined. After stimulation with TNP-LPS, more plasma cells were differentiated in the spleens of mice of both genotypes. Notably, in response to TNP-LPS immunization, β-arr2$^{-/-}$ mice formed even more plasma cells than WT mice, confirming that the absence of β-arr2 aggravates the humoral response (Fig. 4a, b). Consistent with the increased differentiation of plasma cells, deficiency of β-arr2 further facilitated the production of both subtypes of antibodies in the mouse serum despite increases in IgG1 and IgG2A secretion in both immunized WT and β-arr2$^{-/-}$ mice (Fig. 4c, d).

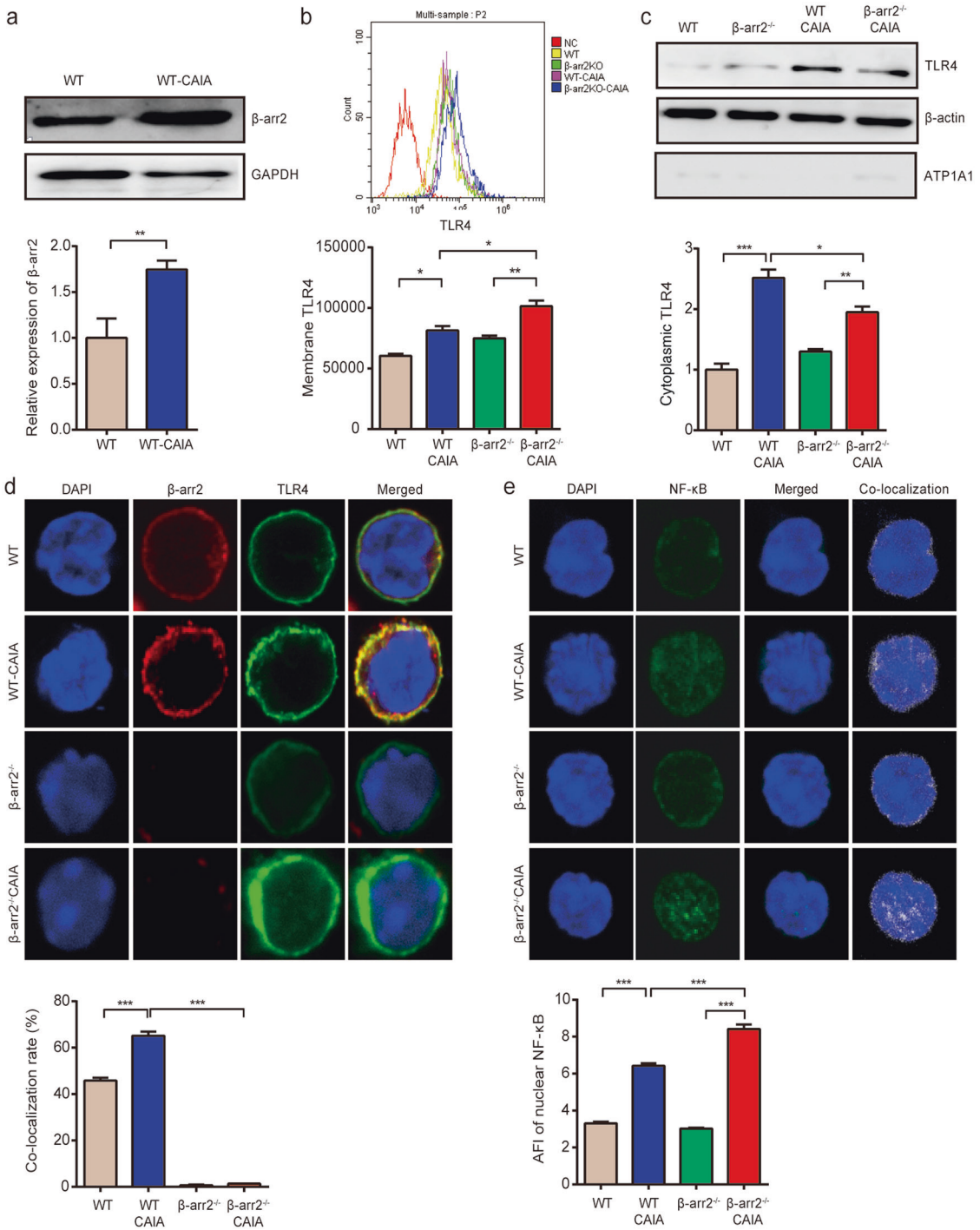

Fig. 3 β-arr2 depletion enhances TLR4-mediated signaling in B lymphocytes of mice with CAIA. a The relative expression of β-arr2 in splenic B lymphocytes from WT control mice and WT mice with CAIA. The intensity of the Western blot bands was analyzed by ImageJ software. **b** Membrane TLR4 expression on B lymphocytes was detected by flow cytometry, and cells only labeled with secondary antibody were used as negative controls. **c** Cytoplasmic TLR4 expression was determined using cytosolic proteins extracted from B lymphocytes by ultracentrifugation, and ATP1A1 was used to evaluate the purity of the isolated cytosolic fractions. **d** The interaction between β-arr2 and TLR4 was assessed by immunofluorescence, and the colocalization rate (%) was analyzed using the built-in software of the confocal microscope. **e** The mean fluorescence intensity of NF-κB p65 in the nucleus was measured as an indicator of the activity of NF-κB. $^{*}P < 0.05$, $^{**}P < 0.01$, $^{***}P < 0.001$ ($n = 5$).

β-arr2 deficiency facilitates LPS-induced B lymphocyte activation, differentiation, and antibody production

The flow cytometry results showed that in vitro LPS stimulation induced the differentiation of splenic B lymphocytes from both WT and β-arr2$^{-/-}$ mice into plasma cells and memory B cells in the spleen. Significantly more plasma cells and memory B cells were generated from β-arr2$^{-/-}$ B lymphocytes than from WT B lymphocytes upon LPS treatment (Fig. 5a–d). The mRNA expression of Blimp1, which controls the differentiation of plasma cells, was markedly upregulated in LPS-stimulated splenic B

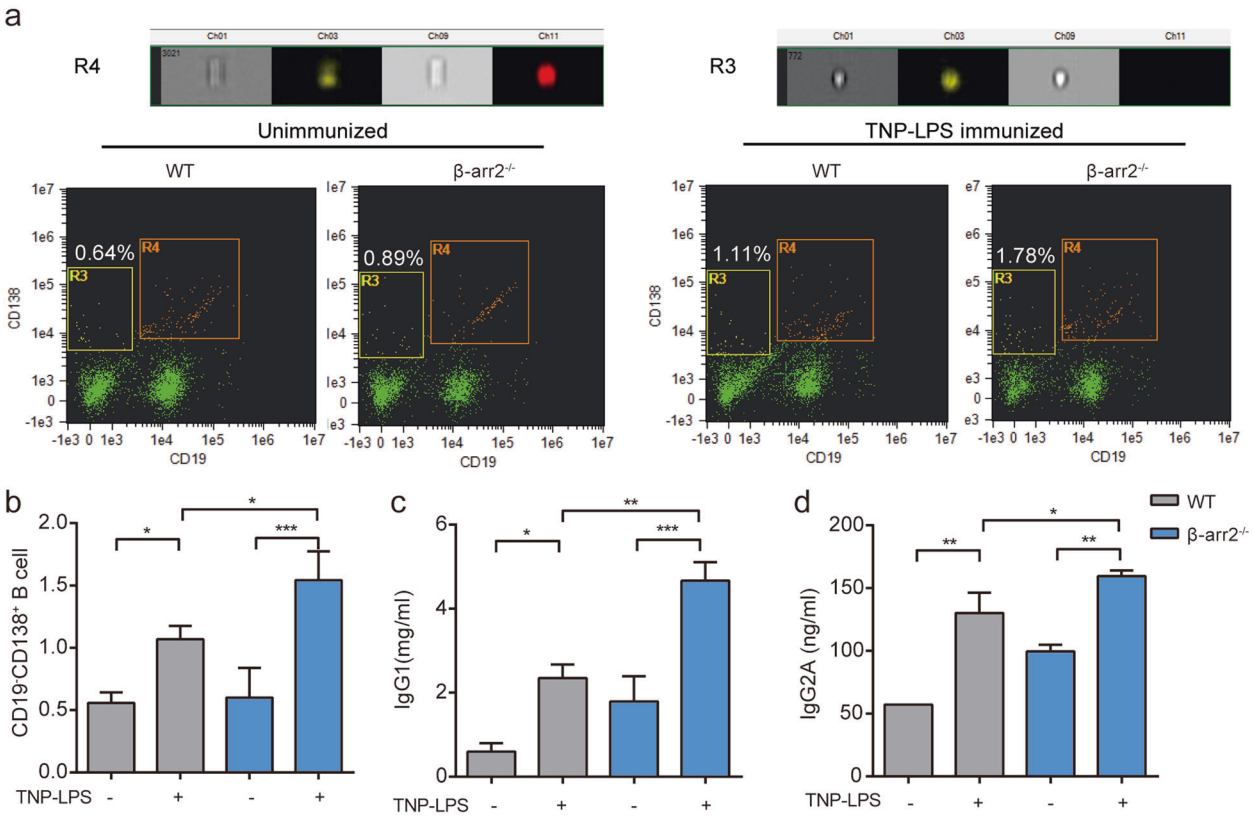

Fig. 4 Loss of β-arr2 aggravates the TNP-LPS-induced humoral response in vivo. a Representative flow cytometry images and the scatter plot of plasma cells are shown. **b** The percentage of plasma cells was analyzed. **c** Serum IgG1 levels (mg/mL) were determined by ELISA. **d** Serum IgG2A levels (ng/mL) were determined by ELISA. $^{*}P < 0.05$, $^{**}P < 0.01$, $^{***}P < 0.001$ ($n = 5$).

lymphocytes from WT or β-arr2$^{-/-}$ mice. It was more significantly expressed in β-arr2$^{-/-}$ B lymphocytes (Fig. 5e). LPS prominently promoted the viability splenic B lymphocytes from mice of both genotypes and induced a more robust response from β-arr2$^{-/-}$ B lymphocytes (Fig. 5f). Combined treatment with LPS and IL-4 is used to induce IgG1 synthesis, while simultaneous administration of LPS and IFN-γ is normally applied to trigger IgG2A production in B lymphocytes [24, 25]. While there was a mild increase in IgG1 production in stimulated WT B lymphocytes, there was a substantial increase in IgG1 synthesis in the supernatant of stimulated β-arr2$^{-/-}$ B lymphocytes, resulting in a significant difference in IgG1 levels between the groups (Fig. 5g). Exposure to LPS and IFN-γ enhanced IgG2A generation in B lymphocytes from mice of both genotypes, and there was a further increase in IgG2A generation in B lymphocytes from β-arr2$^{-/-}$ mice (Fig. 5h). These data proved that β-arr2 is directly involved in plasma cell maturation and antibody production both in vivo and in vitro.

Depletion of β-arr2 retains TLR4 on the plasma membrane and facilitates its downstream NF-κB signaling in B lymphocytes

Isolated B lymphocytes were treated with or without LPS in vitro. Total TLR4 expression was obviously elevated in response to LPS stimulation; however, there was no significant difference between LPS-treated WT and β-arr2$^{-/-}$ B lymphocytes (Fig. 6a). As observed in in vivo studies, LPS induced higher colocalization of TLR4 and β-arr2 in WT B lymphocytes but not in β-arr2$^{-/-}$ B lymphocytes (Fig. 6b). This increased interaction between molecules in LPS-stimulated WT B lymphocytes resulted in endocytosis of TLR4 into the cytoplasm, which was blocked by knocking out β-arr2 in B lymphocytes (Fig. 6c, d). Accordingly, intranuclear NF-κB p65 signaling was found to be much stronger in LPS-treated β-arr2$^{-/-}$ B lymphocytes than in LPS-treated WT B lymphocytes (Fig. 6e). These data suggest that β-arr2 deficiency may promote mitogen-induced plasma cell differentiation by maintaining the membrane distribution of TLR4 and aggravating downstream NF-κB signaling, leading to exacerbation of inflammatory arthritis. Conversely, β-arr2 may help to protect B lymphocytes from overactivation and prevent excessive expansion of plasma cells under inflammatory stimulation, which indicates that it may be an important target for treating humoral immunity-related immune diseases.

DISCUSSION

Although RA is an autoimmune disease involving both abnormal cellular and humoral immune responses, as research on the pathogenesis of RA has progressed, accumulating evidence has shown that overactivation of B lymphocytes, excessive differentiation of plasma cells and the production of a large amount of autoantibodies play important roles in the onset and development of RA [26]. Approximately 70%–80% of RA patients exhibit a higher number of plasma cells and higher anti-CCP levels and RF production than normal subjects as well as a significant correlation between plasma cells and RF levels [27]. In addition, infiltration of plasma cells is found in the synovium of RA patients, and circulating and synovial autoantibodies lead to global and local tissue damage by activating the complement system [28]. Thus, restricting the formation of superabundant plasma cells and corresponding autoantibodies is a promising strategy for treating RA and other autoimmune diseases characterized by humoral immunity dysfunction.

TLR4 initiates the innate immune response to defend against invading pathogens; however, it has also been reported to play a pivotal role in the differentiation of autoreactive B lymphocyte into plasma cells mainly through activating NF-κB signaling and thus contribute to the pathogenesis of autoimmune diseases [28]. Here, we found that injection of antibodies and LPS increases the

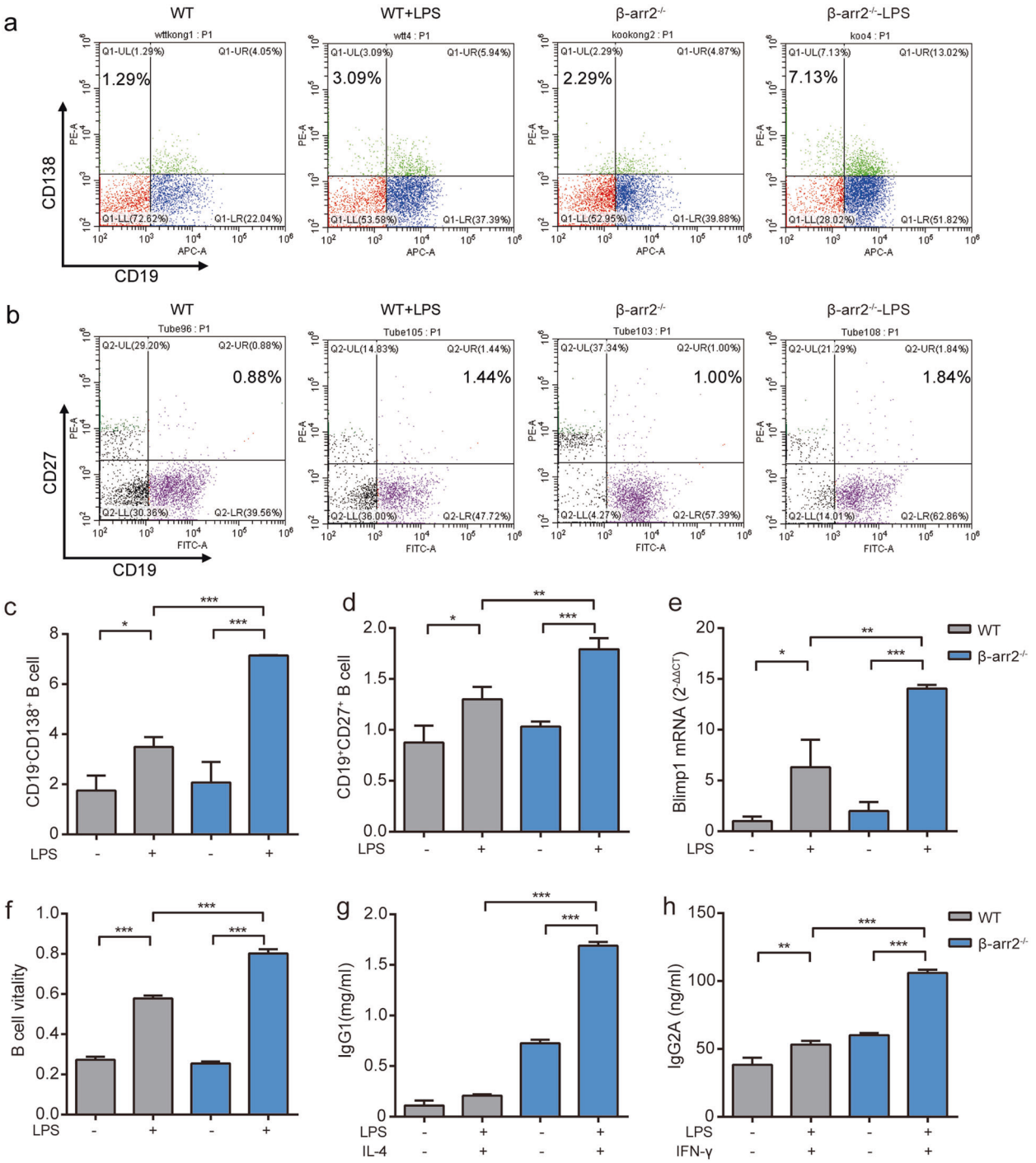

Fig. 5 β-arr2 deficiency facilitates LPS-induced B lymphocyte activation, differentiation, and antibody production. a A representative flow cytometry scatter plot of plasma cells after 72 h of LPS (20 mg/L) stimulation of isolated B lymphocytes is shown. **b** A representative flow cytometry scatter plot of memory B cells after LPS stimulation of isolated B lymphocytes is shown. **c** The percentage of plasma cells was analyzed. **d** The percentage of memory B cells was analyzed. **e** mRNA expression of Blimp1 was quantified using the delta-delta CT method by real-time qPCR. **f** The vitality of B lymphocytes was detected by the CCK-8 assay. **g** IgG1 levels in the culture supernatant of B lymphocytes culture treated with LPS and IL-4 were analyzed. **h** The IgG2A concentration in the culture supernatant of B lymphocytes treated with LPS and IFN-γ was tested. $^{*}P < 0.05$, $^{**}P < 0.01$, $^{***}P < 0.001$ ($n = 5$).

formation of plasma cells, the generation of antibodies, and intranuclear NF-κB activity in B lymphocytes, which manifests as increased NF-κB p65 translocation into the nucleus. Therefore, limiting overactivated TLR4-mediated signaling is beneficial for abolishing the extreme humoral response in autoimmune diseases. In response to LPS stimulation, we observed a clear increase in TLR4 expression in B lymphocytes, most of which was distributed on the plasma membrane to receive continuous stimulation by LPS and to transform the downstream proinflammatory pathway, leading to persistent excessive NF-κB activation and plasma cell differentiation. It has been reported that upon sustained exposure to ligands, TLR4-mediated signaling is negatively regulated by the gradual internalization of activated TLR4, like many other receptors, from the plasma membrane to

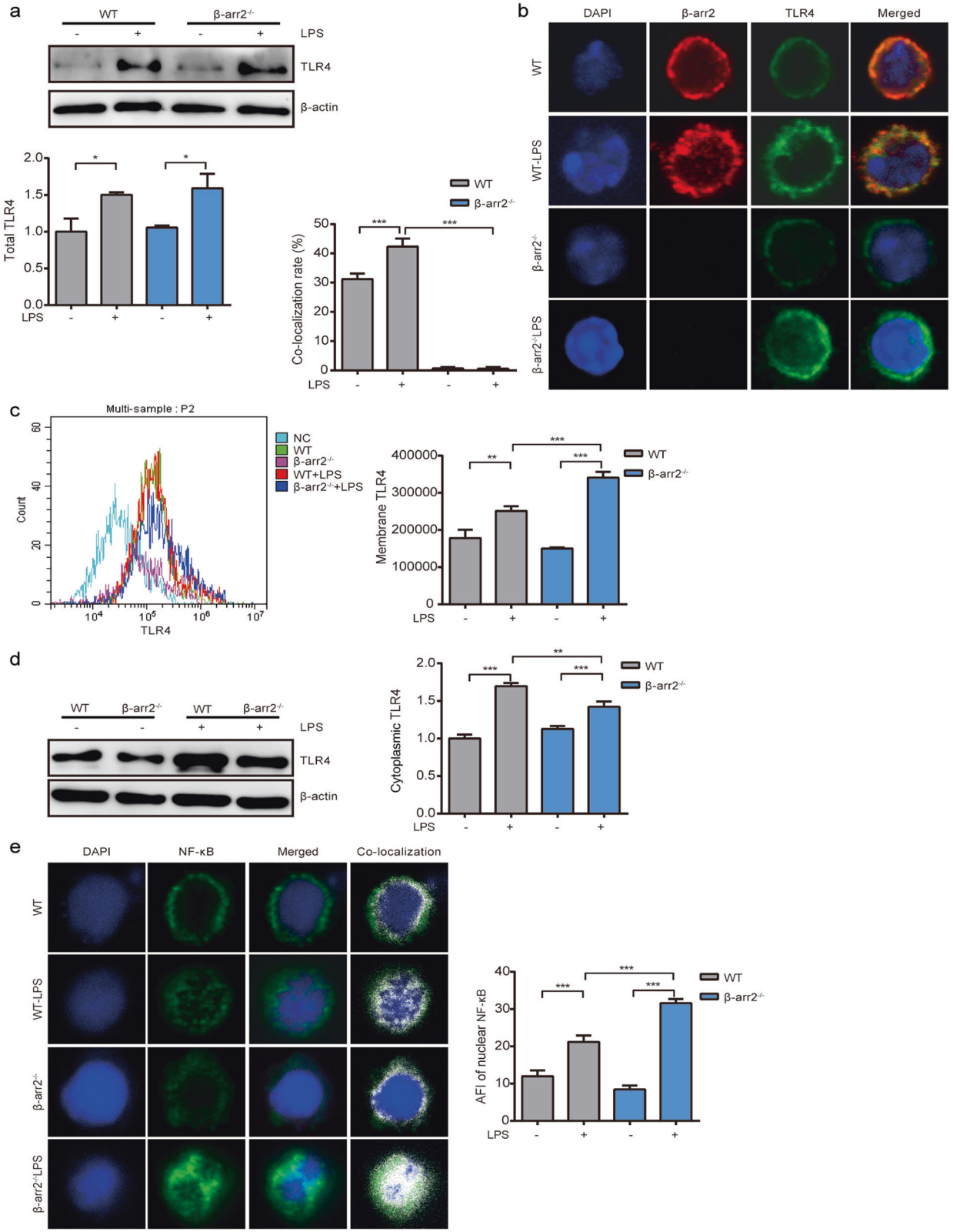

Fig. 6 Depletion of β-arr2 retains TLR4 on the plasma membrane and facilitates downstream NF-κB signaling in B lymphocytes. a Total protein expression of TLR4 in splenic B lymphocytes from WT or β-arr2$^{-/-}$ mice treated with LPS was determined and quantified. **b** The colocalization of β-arr2 and TLR4 in LPS-treated WT or β-arr2$^{-/-}$ B lymphocytes was assessed. **c** Membrane TLR4 expression on B lymphocytes in response to LPS treatment was detected by flow cytometry. **d** Cytoplasmic TLR4 expression was determined using cytosolic proteins extracted from B lymphocytes by ultracentrifugation. **e** The mean fluorescence intensity of NF-κB p65 in the nucleus was analyzed by immunofluorescence. *$P < 0.05$, **$P < 0.01$, ***$P < 0.001$ ($n = 5$).

control the magnitude and duration of the immune response [29]. Endocytosed TLR4 then undergoes ubiquitination and degradation in lysosomes to shut down the signaling pathway.

Multiple mechanisms that regulate TLR4 endocytosis have been revealed. CD14, which is a pattern recognition receptor, has been reported to be essential for LPS-induced TLR4 internalization through Syk/phospholipase Cγ2 signaling and to subsequently regulate the maturation of dendritic cells [30]. However, during endotoxin tolerance, the TLR4 stimulators UT12 and 1Z105 are able to induce receptor endocytosis independent of CD14 in macrophages [11]. Therefore, the mechanisms of TLR4 internalization vary in different types of cells. In addition, evidence has shown that internalization of TLR4 from the membrane is mediated by clathrin, which forms clathrin-coated pits to uptake TLR4 under the coordination of adapter proteins, mainly β-arr2, an adapter protein that has been shown to internalize GPCRs [31]. In the present work, we revealed for the first time that β-arr2 deficiency distinctly promotes the membrane distribution of TLR4, indicating that β-arr2 may be involved in the endocytosis of TLR4 in response to continuous LPS stimulation. CD14-mediated signaling may initiate the process of TLR4 endocytosis; however, clathrin forms clathrin-coated pits and executes receptor trafficking. β-arr2 is an established adapter protein for clathrin and is essential for receptor clustering. The functions of CD14 and β-arr2 in the process of TLR4 internalization are distinct. Colocalization of TLR4 and β-arr2 was observed upon LPS stimulation, indicating that the direct interaction between these two molecules may be involved in the process of TLR4 endocytosis. However, the binding pattern between TLR4 and β-arr2 needs to be further elucidated. When TLR4 internalization was inhibited, nuclear NF-κB translocation was enhanced in β-arr2$^{-/-}$ B lymphocytes and ultimately led to plasma cell differentiation. Therefore, β-arr2 exerts anti-inflammatory effects by terminating the TLR4-triggered hyperinflammatory response through facilitating receptor endocytosis.

Since TLR4 and β-arr2 are comprehensively expressed by multiple immune cells, especially T lymphocytes and macrophages, the anti-inflammatory action of β-arr2 may regulate TLR4 signaling in these cells. In β-arr2$^{-/-}$ mice with CAIA, we observed high Th17 cell generation (data not shown); however, the role of β-arr2 in controlling T cell vitality and the differentiation of Th17 cells is worth investigating. Since B lymphocyte activation is basically T cell-dependent, to confirm the direct role of β-arr2 in humoral immunity, we challenged mice with TNP-LPS, which is used to investigate the T cell-independent B lymphocyte immune response to LPS. Our data demonstrated that upon stimulation with TNP-LPS, more plasma cells differentiated in the spleens of mice of both genotypes. More plasma cells and IgG1 and IgG2A antibodies were produced in β-arr2$^{-/-}$ mice than in WT mice in response to TNP-LPS immunization, confirming that disruption of β-arr2 aggravates the humoral response. Therefore, loss of β-arr2 evokes T cell-independent plasma cell formation and directly accelerates the pathogenesis of joint inflammation. However, expansion of both plasma cells and Th17 cells in β-arr2$^{-/-}$ mice contributes to the exacerbation of inflammatory arthritis; thus, β-arr2 has anti-inflammatory properties in rheumatoid arthritis. The protective role of β-arr2 in colitis and neuroinflammatory diseases such as PD and infection has been addressed [32–34]. Thus, promoting the activation and function of β-arr2 is a promising target for various inflammatory diseases; however, no specific activators or inhibitors of β-arr2 have been successfully designed due to the flexible structure of β-arr2. Thus, indirect regulation of its activity may be an alternative method to modify β-arr2.

CONCLUSION

In conclusion, β-arr2 plays an important role in B lymphocyte differentiation by regulating TLR4-NF-κB signaling in the pathological progression of CAIA. β-arr2 depletion exacerbates CAIA and further increases plasma cell differentiation and antibody production in mice with CAIA. Conversely, these findings suggest that β-arr2 exerts anti-inflammatory effects by terminating the TLR4-triggered hyperinflammatory response through facilitating receptor endocytosis. These results offer a theoretical basis for further elucidating the occurrence and development of RA and provide experimental evidence for the development of β-arr2 as a novel therapeutic target for highly selective therapy for RA.

ACKNOWLEDGEMENTS

This work was supported by the National Natural Science Foundation of China (81202541, 81973332, 81973314), the Anhui Provincial Natural Science Foundation for Distinguished Young Scholars (1808085J28), the Key Projects of Natural Science Research of Anhui Colleges and Universities (KJ2017A176), Anhui University Excellent Youth Talent Support Program (gxyqZD2017025), Innovation and Entrepreneurship Support Program for Returnees of Anhui Province, the Foundation for Young Academic Backbone of Anhui Medical University, and the Grants for Young Talents of Anhui Medical University (2013).

AUTHOR CONTRIBUTIONS

WJZ, DDW, JT, YT, ZWZ, ZW, PPG, WYS, JYC, HXW, SXY and LLZ conducted the study and analyzed the data, WJZ, QTW and WW analyzed the data and wrote the paper.

ADDITIONAL INFORMATION

The online version of this article (https://doi.org/10.1038/s41401-020-00507-1) contains supplementary material, which is available to authorized users.

Competing interests: The authors declare no competing interests.

REFERENCES

1. Wang QT, Wang LS, Wu L, Zhang M, Hu SS, Wang R, et al. Paroxetine alleviates T lymphocyte activation and infiltration to joints of collagen-induced arthritis. Sci Rep. 2017;7:e45364.
2. Han L, Zhang XZ, Wang C, Tang XY, Zhu Y, Cai XY, et al. IgD-Fc-Ig fusion protein, a new biological agent, inhibits T cell function in CIA rats by inhibiting IgD-IgDR-Lck-NF-kappaB signaling pathways. Acta Pharmacol Sin. 2020;41:800–12.
3. Fert-Bober J, Darrah E, Andrade F. Insights into the study and origin of the citrullinome in rheumatoid arthritis. Immunol Rev. 2020;294:133–47.
4. Volkov M, van Schie KA, van der Woude D. Autoantibodies and B cells: the ABC of rheumatoid arthritis pathophysiology. Immunol Rev. 2020;294:148–63.
5. Shu JL, Zhang XZ, Han L, Zhang F, Wu YJ, Tang XY, et al. Paeoniflorin-6′-O-benzene sulfonate alleviates collagen-induced arthritis in mice by down-regulating BAFF-TRAF2-NF-kappaB signaling: comparison with biological agents. Acta Pharmacol Sin. 2019;40:801–13.
6. Wang QT, Ma Y, Liu DD, Zhang LL, Wei W. The roles of B cells and their interactions with fibroblast-like synoviocytes in the pathogenesis of rheumatoid arthritis. Int Arch Allergy Immunol. 2011;155:205–11.
7. Meffre E, O'Connor KC. Impaired B-cell tolerance checkpoints promote the development of autoimmune diseases and pathogenic autoantibodies. Immunol Rev. 2019;292:90–101.
8. Hwang IY, Park C, Harrison K, Kehrl JH. TLR4 signaling augments B lymphocyte migration and overcomes the restriction that limits access to germinal center dark zones. J Exp Med. 2009;206:2641–57.
9. Dekkers JS, Schoones JW, Huizinga TW, Toes RE, van der Helm-van Mil AH. Possibilities for preventive treatment in rheumatoid arthritis? Lessons from experimental animal models of arthritis: a systematic literature review and meta-analysis. Ann Rheum Dis. 2017;76:458–67.
10. Liu G, Lu Y, Shi L, Ren Y, Kong J, Zhang MY, et al. TLR4-MyD88 signaling pathway is responsible for acute lung inflammation induced by reclaimed water. J Hazard Mater. 2020;396:e122586.
11. Rajaiah R, Perkins DJ, Ireland DD, Vogel SN. CD14 dependence of TLR4 endocytosis and TRIF signaling displays ligand specificity and is dissociable in endotoxin tolerance. Proc Natl Acad Sci USA. 2015;112:8391–6.
12. Wang R, Zhang M, Hu SS, Liu KK, Tai Y, Tao J, et al. Ginsenoside metabolite compound-K regulates macrophage function through inhibition of beta-arrestin2. Biomed Pharmacother. 2019;115:e108909.

13. Sun S, Cao H, Yao N, Zhao L, Zhu X, Ni EA, et al. Beta-Arrestin 2 mediates arginine vasopressin-induced IL-6 induction via the ERK1/2-NF-kappaB signal pathway in murine hearts. Acta Pharmacol Sin. 2020;41:198–207.
14. Alexander RA, Lot I, Enslen H. Methods to characterize protein interactions with beta-arrestin in cellulo. Methods Mol Biol. 2019;1957:139–58.
15. Wang QT, Zhang LL, Wu HX, Wei W. The expression change of beta-arrestins in fibroblast-like synoviocytes from rats with collagen-induced arthritis and the effect of total glucosides of paeony. J Ethnopharmacol. 2011;133:511–6.
16. Li H, Smalligan DA, Xie N, Javer A, Zhang Y, Hanley G, et al. Beta-arrestin 2-mediated immune suppression induced by chronic stress. Neuroimmunomodulation. 2011;18:142–9.
17. Li P, Cook JA, Gilkeson GS, Luttrell LM, Wang L, Borg KT, et al. Increased expression of beta-arrestin1 and 2 in murine models of rheumatoid arthritis: isoform specific regulation of inflammation. Mol Immunol. 2011;49:64–74.
18. Fernandez-Zafra T, Gao T, Jurczak A, Sandor K, Hore Z, Agalave NM, et al. Exploring the transcriptome of resident spinal microglia after collagen antibody-induced arthritis. Pain. 2019;160:224–36.
19. Liu KK, Wang Q, Yang SM, Chen J, Wu HX, Wei W. Ginsenoside compound K suppresses the abnormal activation of T lymphocytes in mice with collagen-induced arthritis. Acta Pharmacol Sin. 2014;35:599–612.
20. Clavel G, Marchiol-Fournigault C, Renault G, Boissier MC, Fradelizi D, Bessis N. Ultrasound and Doppler micro-imaging in a model of rheumatoid arthritis in mice. Ann Rheum Dis. 2008;67:1765–72.
21. Huang B, Wang Q, Song S, Wu YJ, Ma Y, Zhang LL, et al. Combined use of etanercept and MTX restores CD4+/CD8+ ratio and Tregs in spleen and thymus in collagen-induced arthritis. Inflamm Res. 2012;61:1229–39.
22. Rui L, Healy JI, Blasioli J, Goodnow CC. ERK signaling is a molecular switch integrating opposing inputs from B cell receptor and T cell cytokines to control TLR4-driven plasma cell differentiation. J Immunol. 2006;177:5337–46.
23. Turner VM, Mabbott NA. Ageing adversely affects the migration and function of marginal zone B cells. Immunology. 2017;151:349–62.
24. Wang J, Liu SC, Hou BD, Yang MX, Dong ZJ, Qi H, et al. PTEN-regulated AID transcription in germinal center B cells is essential for the class-switch recombination and IgG antibody responses. Front Immunol. 2018;9:e371.
25. Leibler C, Thiolat A, Henique C, Samson C, Pilon C, Tamagne M, et al. Control of humoral response in renal transplantation by belatacept depends on a direct effect on B cells and impaired T follicular helper-B cell crosstalk. J Am Soc Nephrol. 2018;29:1049–62.
26. Wang QT, Wu YJ, Huang B, Ma Y, Song S, Zhang LL, et al. Etanercept attenuates collagen-induced arthritis by modulating the association between BAFFR expression and the production of splenic memory B cells. Pharmacol Res. 2013;68:38–45.
27. Derksen V, Huizinga T, van der Woude D. The role of autoantibodies in the pathophysiology of rheumatoid arthritis. Semin Immunopathol. 2017;39:437–46.
28. Lewis MJ, Barnes MR, Blighe K, Goldmann K, Rana S, Hackney JA, et al. Molecular portraits of early rheumatoid arthritis identify clinical and treatment response phenotypes. Cell Rep. 2019;28:2455–70.
29. Shah M, Kim GY, Achek A, Cho EY, Baek WY, Choi YS, et al. The alphaC helix of TIRAP holds therapeutic potential in TLR-mediated autoimmune diseases. Biomaterials. 2020;245:e119974.
30. Zanoni I, Ostuni R, Marek LR, Barresi S, Barbalat R, Barton GM, et al. CD14 controls the LPS-induced endocytosis of Toll-like receptor 4. Cell. 2011;147:868–80.
31. Pascual-Lucas M, Fernandez-Lizarbe S, Montesinos J, Guerri C. LPS or ethanol triggers clathrin- and rafts/caveolae-dependent endocytosis of TLR4 in cortical astrocytes. J Neurochem. 2014;129:448–62.
32. Sharma D, Malik A, Steury MD, Lucas PC, Parameswaran N. Protective role of beta-arrestin2 in colitis through modulation of T-cell activation. Inflamm Bowel Dis. 2015;21:2766–77.
33. Feng X, Wu C, Burton FH, Loh HH, Wei L. Beta-arrestin protects neurons by mediating endogenous opioid arrest of inflammatory microglia. Cell Death Differ. 2014;21:397–406.
34. Sharma D, Parameswaran N. Multifaceted role of beta-arrestins in inflammation and disease. Genes Immun. 2015;16:e576.